Simulation of the gas density distribution in the accelerator of the ELISE test facility

M. Siragusa,[1,2,a)] E. Sartori,[1,2] F. Bonomo,[3] B. Heinemann,[3] G. Orozco,[3] and G. Serianni[1]
[1)] *Consorzio RFX, Corso Stati Uniti 4, 35127 Padova (PD), Italy*
[2)] *Università degli Studi di Padova, Via 8 Febbraio 2, I-35122 Padova (PD), Italy*
[3)] *Max-Planck-Institut für Plasmaphysik, Boltzmannstraße 2, 85748 Garching, Germany*

In multi-aperture electrostatic accelerators of negative ion sources, the plasma discharge is sustained by injecting gas in the plasma source, in a dynamic equilibrium with the gas flowing out through the accelerator. In this work we present a three-dimensional numerical simulation of the gas flow inside the accelerator system of the large negative ion source ELISE at IPP Garching. ELISE has 640 apertures per electrode and lateral gaps between the electrode support structures that also contribute to the total gas conductance. Assuming molecular regime we estimated the gas conductance, the gas density profile along the path of the ion beams from upstream of the plasma grid to downstream of the ground grid, and the transverse non-uniformities in the accelerator. The simulation included the most relevant geometrical features, while the results are compared to analytical results.

Keywords: Pressure distribution, 3D simulation, large negative ion source

I. INTRODUCTION

Two Neutral Beam Injector (NBI) lines are foreseen to provide a total power of 33 MW of either 1 MeV D0 or 870 keV H0 into the ITER plasma, for heating and current drive[1]. In each line, the fast neutrals are created as negative particles in a single large RF-driven ion source, extracted and accelerated to the full energy before being neutralized in a gas neutralizer.

The ITER injectors are designed for an accelerated D^- current density of 200 A/m^2 and an accelerated current of 40 A (in the first ITER operation phase, 230 A/m^2 of H^- current density for a total current of 46 A). However, losses of extracted negative ions occur in the extraction system mainly due to electron stripping (i.e. electron detachment of the negative ions before being fully accelerated). To compensate the consequent reduction of beam efficiency, a larger amount of negative ions has to be extracted from the source and accelerated. The estimation of the stripping losses within the extractor and the accelerator of the ITER NBI source has been calculated using the gas density profile along the beam line as obtained with the GasFlow3D code[2]. An acceptable amount of 30 %[3] of stripping losses has been estimated at the operational filling pressure of 0.3 Pa. Similar values have been more recently confirmed also by simulations using a different code for the gas density profile, AVOCADO[4,5,6].

Validation of the predicted stripping losses will be assessed at the ITER NBI full-size 7-stage -acceleration-source MITICA (Megavolt ITER Injector Concept Advanced)[1], which is part of the Neutral Beam Test Facility project PRIMA[1] based at Consorzio RFX, Padua currently under construction. The stripping losses in other ITER-like negative ion source test facilities such as SPIDER[7,8] or ELISE[9,10] (see Fig. 1), are studied to get an earlier insight, although they are based on an only 3-stage acceleration system. SPIDER is the full-size ITER NBI source, with a maximum acceleration potential of 100 kV. ELISE is the half-size of the ITER NBI source (but same width), with a maximum acceleration potential of 60 kV.

In this work, we focused on the calculation of the gas pressure profiles in the multi-aperture multi-grid accelerator of ELISE. We expect that numerical calculations can provide an accurate estimation of the spatial distribution of background gas density in the electrostatic accelerator. As the accelerator is immersed in vacuum, it is expected that a pumping effect towards the sides is present, with an possible difference in terms of background gas density and therefore a lower stripping loss for the edge beamlets. Specifically in the case of ELISE, the large number of apertures (640) and the transverse dimensions of the electrodes (approx. 0.8 m) will exacerbate this effect with respect to smaller prototype ion sources. One of the purposes of this paper is therefore to clarify the entity of this effect.

In addition to the estimation of macroscopic transversal non uniformities, numerical calculations can provide a well-resolute axial profile. In the first few centimeters of the accelerator of ELISE, the distance between the electrodes is smaller than the aperture diameter. If we take the latter as a characteristic length for the perturbation to an undisturbed gas flow field before and after an aperture, one can see that the assumption of uniform gas pressure in between the grids may not be a satisfying approximation. In this context numerical simulations can contribute to an improved estimation.

The calculations presented in this work are performed at room temperature, and simulate the filling condition of the ELISE beam source for the first time. The simula-

[a)] Electronic mail: marco.siragusa@igi.cnr.it

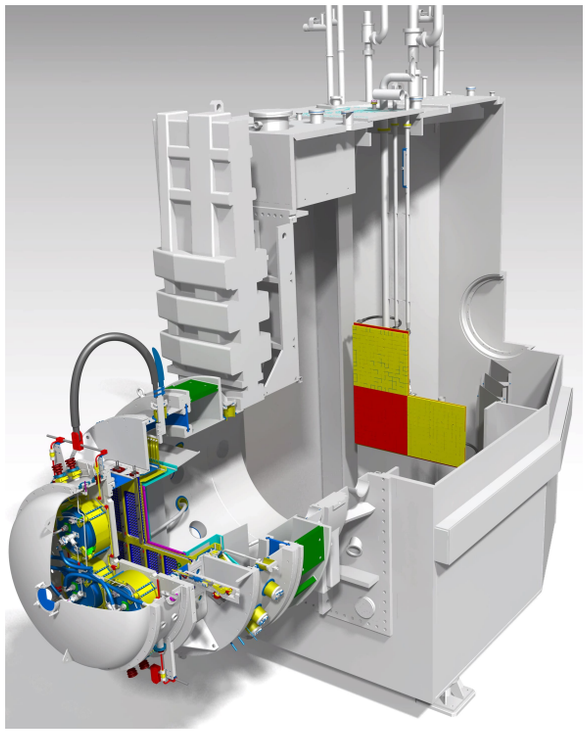

FIG. 1. Isometric view of ELISE facility

tions were positively benchmarked to experimental data on the basis of measured pressures and measured gas throughput, in order to validate the simulation by the checking the overall gas conductance for the system. The calculations at room temperature and related benchmark are considered a fundamental step towards the study of operating conditions, which shall include additional effects to the gas such as gas heating by the plasma, dissociation, and so on.

II. GEOMETRY AND MODEL DESCRIPTION

The gas flow domain is composed by the whole ion source, accelerator and ground support tube to the large vacuum vessel, where two large cryopumps are installed. Fig. 2 sketches the multi-aperture electrostatic accelerator grids and the grid holder boxes. The accelerator consists of three parallel grids, namely Plasma Grid (PG), Extraction Grid (EG) and Grounded Grid (GG), and it is composed by 640 apertures with a minimum size of D12 mm. The spacing between the grids and their grid holder boxes is as small as 6 mm and is also included in the model: an example is shown in Fig. 4. Detailed information on the extraction system geometry are reported by B. Heinemann *et al.*[9] in 2009. The study of the flow domain is complex, therefore, second order geometrical features with minor impact on the overall conductance of the system – such as electrical and hydraulic connectors and pipes – were not considered.

The typical operating source filling pressure of ELISE is 0.3 Pa for hydrogen and deuterium. In such conditions, the gas flow regime at the plasma-grid apertures is of molecular flow, with a Knudsen number $Kn = \lambda/L$ expected to be marginally above unity in all regions with significant pressure gradients. Two approaches are followed to calculate the total conductance. The first combines analytical relations for thin slit approximation with rectangular cross section and cylindrical and conical apertures[11] (in free molecular flow regime) with lumped models. The second is a full three-dimensional numerical model with the AVOCADO code[45]. The code makes use of the mathematical analogy existing between the law of molecular flow and radiative exchange between surfaces. The set of governing equations is derived on the basis of the fact that the geometry dominates molecular flow, and that the pressure distribution is obtainable by surface discretization and calculation of mutual exchanges due to molecular trajectories. The pressure at the surface is defined by Eq. (1). The cosine law can be used to obtain a "view factor" $F_{i,j}$ between any pair of surface elements (see Eq. (2)). The balance of net particle exchange between two surface elements can be generalized with the Eq. (3).

$$p = \phi \cdot (2\pi m k_B T)^{1/2} \tag{1}$$

$$F_{i,j} = F_{j,i} = \int F_{i \to j} \cdot d\Sigma_i \tag{2}$$

$$\phi_{net,i,j} = (\phi_i - \phi_j) \cdot F_{i,j} \tag{3}$$

In the molecular flow regime, the mathematical problem is linear, so the study is calculated once at a normalized source pressure, and then rescaled to values relevant for ELISE operation. As boundary conditions, the pressure is defined at the back plates of all four drivers, and at a virtual surface at the entrance of the large vacuum tank and the ground support tube. This boundary condition definition assures the least influence on the simulation results for their distance from the region of strong pressure gradient (accelerator grids).

Two sub-models were developed to separate the gas leaking from the source volume through the small gap around the PG from the gas flow through all apertures of the grids including the lateral gas flow in the accelerator.

The first simplified model, without grid apertures, was used to estimate the conductance of the gap between vessel and PG holder. Conductances of thin slits[11] were combined into C_{gap} using the equivalent circuit sketched in Fig. 3. Similarly, a modified geometry was modelled in AVOCADO and simulated to obtain the numerical C_{gap}.

The second model was used to calculate the accelerator conductance, including grid apertures and lateral gaps through the supporting frames, together with all gaps between these (see Fig. 4). The analytical conductance was estimated considering each beamlet apertures as short tubes with circular cross section, or conical apertures; whereas the gaps between the grid holders was calculated using thin slit approximation with rectangu-

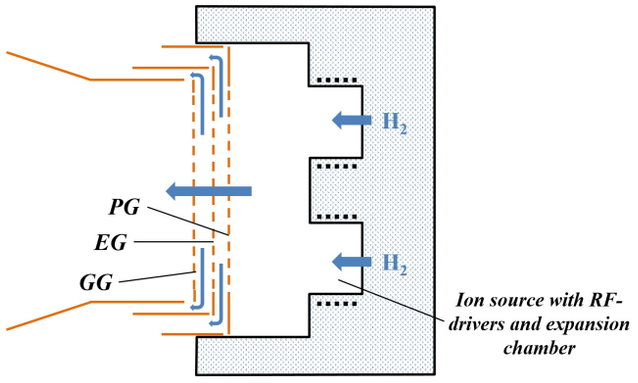

FIG. 2. Sketch of horizontal section view of ELISE ion source and accelerator. The gas flows through the grids and grid holder boxes

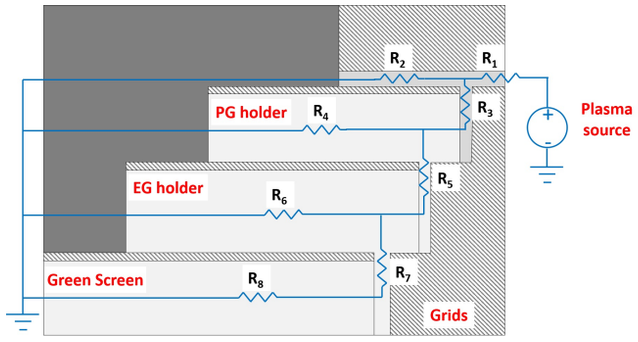

FIG. 3. Simplified electrical model of the gas conductance through the gap between vessel and PG holder, the grids are modelled as a closed wall

lar cross section[11]. The analytical conductances allow to calculate the variation of gas density upstream and downstream each grids, but not the gas density profile, therefore to have the gas density profile is needed to perform numerical simulations.

The three-dimensional simulation was done using the whole domain, which is computationally expensive because the small grid apertures require a fine mesh resolution in the large source dimension. In Fig. 5, a section view of the whole domain used in AVOCADO, from the driver to the vessel downstream the grid system, is shown.

The global conductance C_{tot}, presented in Table I, was calculated by adding the results of the two models as parallel conductances. There is a good agreement between the results calculated with the two methods, numerical and analytical.

The conductance results can be easily presented as pressure difference between the ion source filling pressure and the tank pressure, as shown in Fig. 6 for the hydrogenic species. The numerical results performed for gas and surfaces all at room temperature (300 K) are compared with the experimental data provided by IPP and taken while keeping $T_{wall,\,ion-source} = 40°C$,

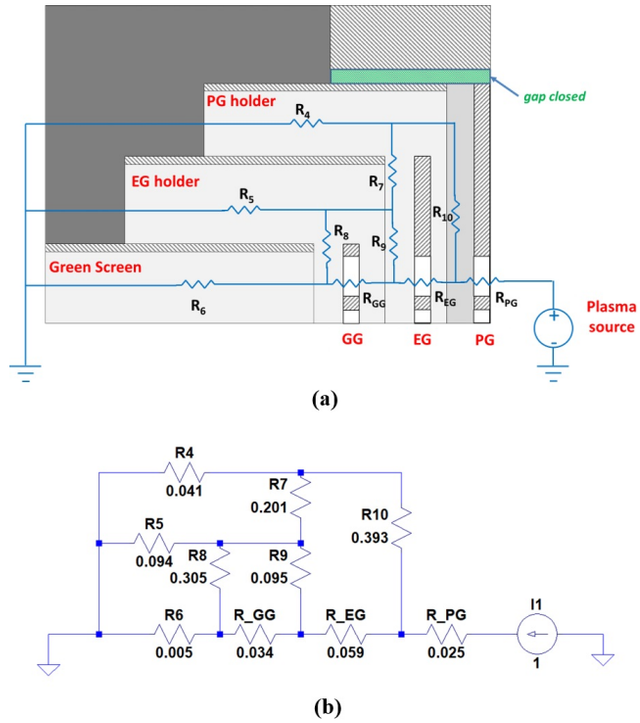

FIG. 4. Simplified electrical model of the gas conductance through the accelerator: (a) lateral section of the grids with their frames; (b) equivalent electric circuit in LTspice®

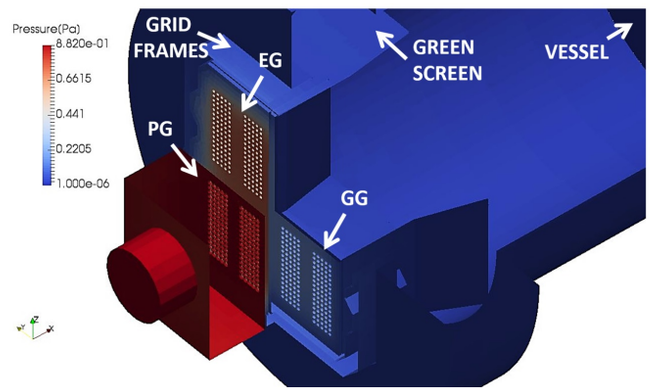

FIG. 5. Section view of the calculation domain used for the three-dimensional gas flow model of ELISE; colour scale indicates pressure distribution

		Numerical simulation	*Analytical calculation*
$C_{grids\ \&\ frames}$	(m^3/s)	10.9	9.8
C_{gap}	(m^3/s)	2.3	2.4
C_{tot}	(m^3/s)	13.2	12.2

TABLE I. Beam source conductance in H_2 at $T = 300\ K$

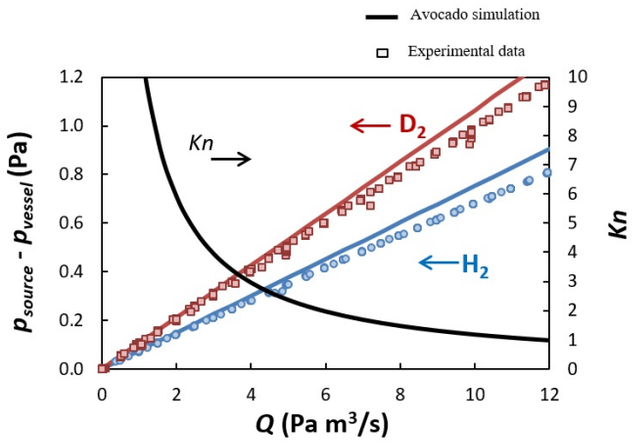

FIG. 6. Difference between source filling pressure and tank pressure (experimental data with symbols, calculation with lines), as a function of the injected throughput Q at 300 K. The correspondent Knudsen number calculated at the PG beamlet aperture is shown on the right-y axis.

$T_{PG} = 125°C$, $T_{EG} = 40°C$. The comparison shows a good coherence between simulation and measurements. The applicability of the molecular approximation is fulfilled up to a source pressure around 1 Pa for both species, because up to that source pressure the Knudsen number is larger than one (see Fig. 6).

III. TRANSVERSAL NON UNIFORMITIES AND AXIAL PROFILES THROUGH THE ACCELERATOR GRIDS

The transversal pressure profiles across the grid surfaces were calculated from the simulation along two horizontal lines, located at the mid-plane of the accelerator and above the beamlet groups at both upstream and downstream sides of the grids as shown in Fig. 7. The resulting pressure profiles are displayed in Fig. 8, for all the three grids. The position of the four rectangular beamlet groups is marked by the rectangular shadowed area. Due to the vertical symmetry of the ELISE source, grids and components, no profiles for the bottom part of the source have been here considered.

Four apertures in the beamlet groups have been selected in Fig. 7 as the more significant ones, and the correspondent pressure profiles in axial direction are presented in Fig. 9. They have been chosen to illustrate the maximum non uniformity of the gas profiles in the ELISE accelerator. In Fig. 9, numerical results from AVOCADO (solid lines) are compared with the profiles that can be calculated in the analytical approximation (dashed line). The analytical profile has been obtained by assigning all the pressure variation to the region within the grid thickness. The assumption that a uniform pressure exists in the volume between the grids, for gaps of a length comparable to the aperture diameter or smaller, is clearly not justified along the beamlet axis. One should notice that

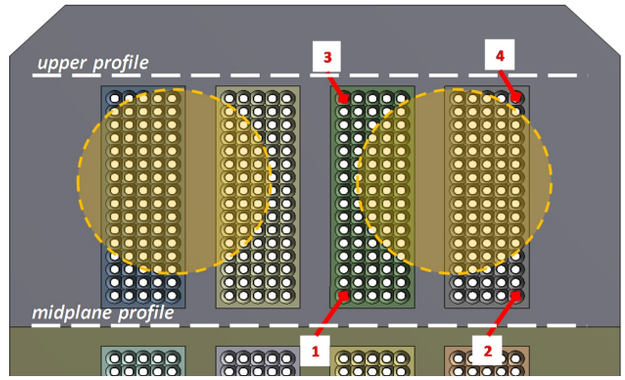

FIG. 7. Positions of axial (x-axis) and transversal (y-axis) profiles, the highlighted circles represents the RF-drivers projections

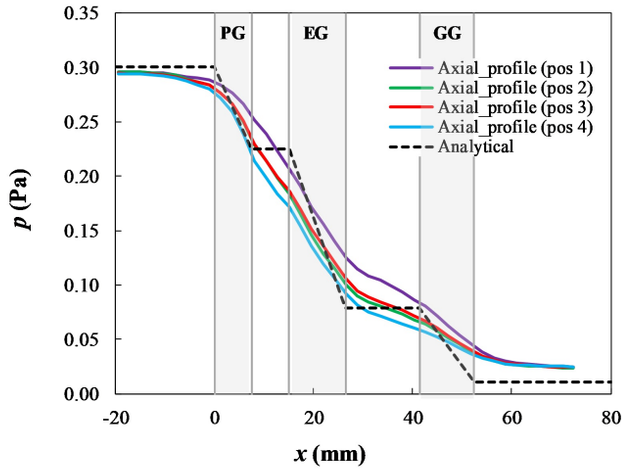

FIG. 8. Calculated pressure profiles along the beamlet paths for the apertures highlighted in Fig. 7, both from AVOCADO (solid lines) and with analytical calculation (dashed line).

changes along the transversal directions cannot be appreciated by the analytical model, which considers only an effective length for rectangular slits considered to calculate the lateral conductances of the accelerator.

IV. CONCLUSIONS

This paper presents the investigations of the gas flow at room temperature in ELISE, in the molecular flow regime, using a full scale three-dimensional domain. The conductance obtained from this simulation is in agreement with the analytical one and with experimental data. The model including full 3D features such as the lateral conductances through the grid holder boxes towards the vacuum tank enabled investigating the transverse uniformity of the gas density in between the accelerator grids.

During plasma discharge in the ion source, the gas

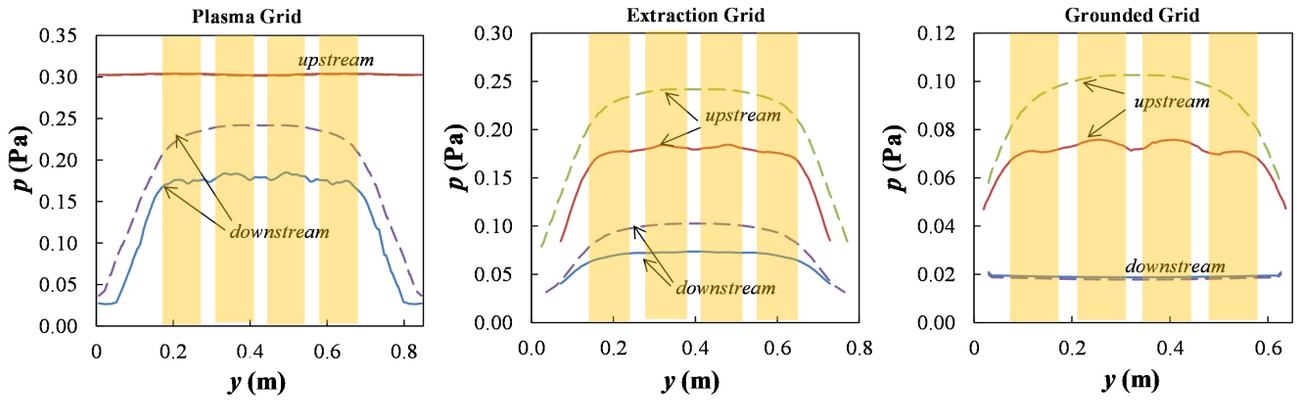

FIG. 9. Pressure transversal profiles upstream and downstream each grid: upper profile (continuous line) and mid plane profile (dashed line); the rectangular yellow shadowed area represent the beamlet groups

has a higher temperature and a dissociation degree non-negligible. Both these factors will influence the gas density distribution in the accelerator structure. In a future work, these factors will be considered in the model by thermal accommodation for all the gas particles and the recombination of hydrogen atoms due to the collisions with accelerator system. This will lead to an estimation of gas density profile closer to real experimental scenario.

[1]R. Hemsworth, D. Boilson, P. Blatchford, M. Dalla Palma, G. Chitarin, H. De Esch, F. Geli, M. Dremel, J. Graceffa, D. Marcuzzi, *et al.*, "Overview of the design of the ITER heating neutral beam injectors," New Journal of Physics **19**, 025005 (2017).

[2]A. Krylov and R. Hemsworth, "Gas flow and related beam losses in the ITER neutral beam injector," Fusion engineering and design **81**, 2239–2248 (2006).

[3]R. Hemsworth, H. Decamps, J. Graceffa, B. Schunke, M. Tanaka, M. Dremel, A. Tanga, H. De Esch, F. Geli, J. Milnes, *et al.*, "Status of the ITER heating neutral beam system," Nuclear Fusion **49**, 045006 (2009).

[4]E. Sartori and P. Veltri, "AVOCADO: A numerical code to calculate gas pressure distribution," Vacuum **90**, 80–88 (2013).

[5]E. Sartori, G. Serianni, and S. Dal Bello, "Simulation of the gas density distribution in the large vacuum system of a fusion-relevant particle accelerator at different scales," Vacuum **122**, 275–285 (2015).

[6]P. Agostinetti, D. Aprile, V. Antoni, M. Cavenago, G. Chitarin, H. De Esch, A. De Lorenzi, N. Fonnesu, G. Gambetta, R. Hemsworth, *et al.*, "Detailed design optimization of the MITICA negative ion accelerator in view of the ITER NBI," Nuclear Fusion **56**, 016015 (2015).

[7]P. a. Sonato, P. Agostinetti, G. Anaclerio, V. Antoni, O. Barana, M. Bigi, M. Boldrin, M. Cavenago, S. Dal Bello, M. Dalla Palma, *et al.*, "The ITER full size plasma source device design," Fusion Engineering and Design **84**, 269–274 (2009).

[8]S. G, "presented at ICIS 2019 China," (2019).

[9]B. Heinemann, H. Falter, U. Fantz, P. Franzen, M. Fröschle, R. Gutser, W. Kraus, R. Nocentini, R. Riedl, E. Speth, *et al.*, "Design of the "half-size" ITER neutral beam source for the test facility ELISE," Fusion Engineering and Design **84**, 915–922 (2009).

[10]D. Wünderlich, R. Riedl, F. Bonomo, I. Mario, U. Fantz, B. Heinemann, W. Kraus, N. Team, *et al.*, "Achievement of ITER-relevant accelerated negative hydrogen ion current densities over 1000 s at the ELISE test facility," Nuclear Fusion **59**, 084001 (2019).

[11]C. B. Nakhosteen and K. Jousten, *Handbook of vacuum technology* (John Wiley & Sons, 2016).